Combination of image processing and artificial neural networks as a novel approach for the identification of *Bemisia tabaci* and *Frankliniella occidentalis* on sticky traps in greenhouse agriculture

Karlos Espinoza, Diego L. Valera*, José A. Torres, Alejandro López, Francisco D. Molina-Aiz

Research Centre CIAMBITAL, University of Almería, Ctra. Sacramento s/n, 04120 Almería, Spain.

Abstract

Integrated Pest Management (IPM) lies at the core of the current efforts to reduce the use of deleterious chemicals in greenhouse agriculture. IPM strategies rely on the early detection and continuous monitoring of pest populations, a critical task that is not only time-consuming but also highly dependent on human judgement and therefore prone to error. In this study, we propose a novel approach for the detection and monitoring of adult-stage whitefly (*Bemisia tabaci*) and thrip (*Frankliniella occidentalis*) in greenhouses based on the combination of an image-processing algorithm and artificial neural networks. Digital images of sticky traps were obtained via an image-acquisition system. Detection of the objects in the images, segmentation, and morphological and color property estimation was performed by an image-processing algorithm for each of the detected objects. Finally, classification was achieved by means of a feed-forward multi-layer artificial neural network. The proposed whitefly identification algorithm achieved high pre-

*Corresponding author. Research Centre CIAMBITAL; Tel.: +34-950-015-546; Fax: +34-950-015-491

Email addresses: ker154@ual.es (Karlos Espinoza), dvalera@ual.es (Diego L. Valera), jtorres@ual.es (José A. Torres), alexlopez@ual.es (Alejandro López), fmolina@ual.es (Francisco D. Molina-Aiz)

cision (0.96), recall (0.95) and F-measure (0.95) values, whereas the thrip identification algorithm obtained similar precision (0.92), recall (0.96) and F-measure (0.94) values.

Keywords: IPM, Early pest detection, Sticky trap, Insect identification, Image processing, Artificial neural network

1. Introduction

The rising public demand for food safety and quality is creating market opportunities for certified products, grown using Integrated Pest Management (IPM) practices (Anderson et al., 1996; Dhawan and Peshin, 2009). Controlling pests in greenhouses has become a complex task that requires an early and precise pest detection strategy (Zhao et al., 2011a). Various non-chemical control methods have been developed (Tang et al., 2005) to keep pest density to a minimum, such as insect-proof screens (Valera et al., 2006; López et al., 2013; Espinoza et al., 2015). In this context, the use of sticky traps to capture insects and monitor pest populations has become a key decision-making tool in a well-planned IPM strategy (Pinto-Zevallos and Vänninen, 2013). Pest population monitoring using sticky traps has traditionally relied on a manual count based on human eyesight (Wise et al., 2015). Although various alternative manual counting strategies have been proposed to decrease the effort and time associated with counting small insects trapped on sticky traps (Heinz et al., 1992; Gerling and Horowitz, 1984; Steiner et al., 1999), the implementation of automatic pest identification systems has become a priority for the development of modern agricultural production systems (Xia et al., 2014).

An automatic pest identification system basically consists of two stages: image acquisition and the image processing algorithm (which, in turn, comprises segmentation, feature extraction and feature classification).

In the image aquisition stage, abiotic factors such as climatic conditions, and greenhouse characteristics and management have to be considered when collecting images from agrosystems, since they affect the efficiency of sticky traps (Isaacs and Byrne, 1998; Teitel et al., 2005; Biffi, 2009; Pérez et al., 2010; Pinto-Zevallos and Vänninen, 2013). Insect sampling has undergone certain innovative technological contributions, such as the mobile suction mechanism proposed by Bauch and Rath (2005) and the 3-degree of freedom robot with a sticky trap and a spray nozzle to remove insects from plants developed by Chung et al. (2014). With a different approach, Li et al. (2009) developed an algorithm to identify the 3-dimensional position of an experimental insect model on plant leaves, whereas Bechar et al. (2010) used an online-video camera for *in-situ* pest monitoring. The quality of the information in the acquired images is important for the performance of an insect identifiaction system. To obtain detailed information of the target insects, high-resolution images have been used (Qiao et al., 2008; Solis-Sánchez et al., 2009; Kumar et al., 2010). In a similar vein, Cho et al. (2007) and Xia et al. (2014) performed several evaluations to find out the optimum image resolution and thus reduce computational cost, which is dependent on the image resolution to be processed. As an alternative, other authors (Huddar et al., 2012; Boissard et al., 2008) opted to acquire close-up images of the target insects. However, the use of close-up images implies an underestimation of the number of identified insects for the full-scale trap (Qiao et al., 2008),

thus requiring an approximation method (Gerling and Horowitz, 1984; Heinz et al., 1992; Steiner et al., 1999).

A growing number of image-processing algorithms have been developed to identify small pests in sticky traps such as whiteflies and thrips. The segmentation process used to detect objects on the trap images was developed using empirical intensity thresholds (Cho et al., 2007; Qiao et al., 2008). These algorithms are simple and accurate. Nevertheless, the empirical parameter must be manually adjusted if the method is used in different image acquisition conditions. Solis-Sánchez et al. (2009) reduced the input empirical parameters used in the insect identification algorithm and used the automatic clustering-based image thresholding method proposed by Otsu (1979). In a similar fashion, Xia et al. (2014) used marker-controlled watershed segmentation.

In the previously mentioned studies, color and shape features were used to identify the objects detected in the segmentation process. Solis-Sánchez et al. (2011) took a different approach based on the use of Scale-Invariant Feature Transform developed by Lowe (2004) and determined that the properties of this feature are invariant to image scale and rotation, and provide robust matching across a substantial range of distortion, noise and illumination. Nevertheless, the classification process of color, shape and invariant features was still performed by comparing detected object features within an empirical domain.

Classification of the extracted features is an important process in an insect identification algorithm. To perform this task, Kumar et al. (2010) proposed using Support Vector Machines to classify the features extracted from the

objects detected in sticky traps. Despite the fact that the segmentation algorithm was tuned to match the highly variable conditions in which video images were acquired, the authors obtained good results using the supervised learning model.

Artificial neural network (ANN) is a supervised learning model that has been used successfully in numerous applications. The model consists of three elements: the set of synapses or connecting links, the adder and the activation function or transfer function (Haykin, 1998). In vision systems, it has been used for image recognition and classification. ANN can be employed to classify the feature vectors extracted after the segmentation process in a variety of application domains. As an example, other supervised learning models have been used in the classification stage of the automatic identification of microorganisms and taxon identification. In the method developed by Ginoris et al. (2007) to identify micro-organisms, they used an *ad hoc* algorithm in the segmentation process to obtain morphological features used for the classification process. After evaluating three classification processes, they concluded that the discriminant analysis and the feed-forward artificial neural network results were similar, whereas the decision trees technique was less appropriate. Likewise, Yaakob and Jain (2012) investigated the use of a Quality Threshold ARTMAP (QTAM) artificial neural network for the classification of six different types of moment invariant features for the recognition of the insect shapes. After comparing it with several Fuzzy ARTMAP neural networks, they found that the highest insect recognition was achieved by classifying the Krawtchouk Moment Invariant features with a QTAM neural network enhanced with the Mahalanobis distance function. Although an un-

certainty factor was found when using normalised moment invariant features with these neural networks for the classification of 20 different types of insect shapes, the algorithm had a high performance.

Artificial neural networks are a good strategy for the classification of insect features since, as opposed to *ad hoc* algorithms, they are not limited in the number of insects that can be classified, they do not require the empirical adjustment of constants, and the upgrade of the classification method is less complex. However, while ANN can be used to identify a wide spectrum of insects, no previous studies have used these models to identify small and less detailed insects on sticky traps.

In this study, we propose to use feed-forward neural networks in combination with an image processing algorithm to identify the most aggressive pests that affect the tomato-producing greenhouses of southern Spain (Acebedo, 2004; CAPDR, 2014), i.e. the whitefly (*Bemisia tabaci*) and thrip (*Frankliniella occidentalis*), both captured using sticky traps. Moreover, an object detection subroutine is proposed to reduce the amount of information to be processed during the segmentation subroutine of the insect identification algorithm. This paper is structured as follows: Section 2.1 and Section 2.2 describe the data acquisition procedure and the developed insect identification algorithm, respectively. The results are then presented and discussed in Section 3. Lastly, our conclusions are drawn in Section 4.

2. Methodology

2.1. Images acquisition

To gather representative experimental data, sticky traps were homogeneously set up in a tomato crop (*Licopersicum sculentum* L. cv Marenza) grown in three multi-span greenhouses and an Almería-type greenhouse located at the research farm of the University of Almería, Spain (36°51′52.4″ N, 2°16′58.5″ W, 87 m.a.s.l). A detailed description of these greenhouses can be found in the studies conducted by López et al. (2012) and Valera et al. (2016).

Adult-stage whitefly (*Bemisia tabaci*) and thrip (*Frankliniella occidentalis*) were selected as the target species for identification. A selective capture of these two insects was performed by using two different models of sticky traps, yellow and blue, for whiteflies and thrips, respectively (Fig. 1). Solid-color traps were used to avoid noise in the digital images caused by grids, as previously reported by other authors (Cho et al., 2007; Xia et al., 2014), or by any other printed marks on the sticky traps. Traps were replaced and moved to the laboratory weekly for data retrieval during 21 weeks of the complete crop cycle (January 22rd to Jun 18th, 2014). As a result of this sampling strategy, we obtained a total of 1593 sticky traps, of which 903 were yellow sticky traps (YST) and 690 were blue sticky traps (BST).

After manual counting was performed using a VTLAMP2WN (Velleman, Gavere, Belgium) magnifying lamp of 5 dpt, the sticky traps were digitalized using a Scoutbox sensor (Cropwatch Company, Wageningen, Netherlands) which consists of a closed box to insulate light conditions and an internal camera (Canon EOS 550D with EF 35 mm f/2 lens model). Thus, a total of

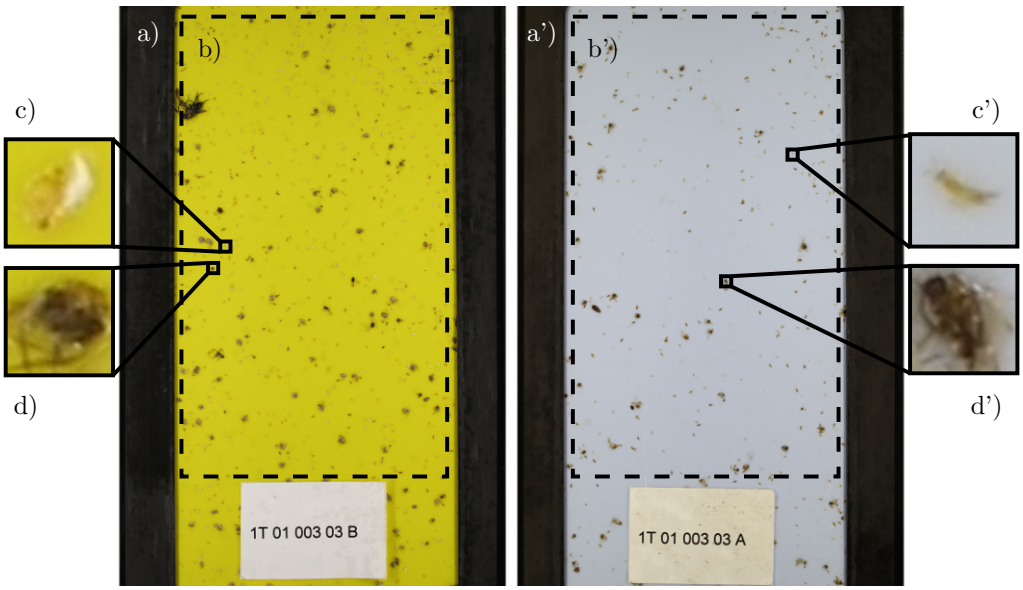

Figure 1: YST and BST used to capture whiteflies and thrips. a) and a') steel frames for the support of the sticky traps; b) and b') area of interes for counting and tagging of target insect and non-target objects; c) and c') whitefly and thrip sample images, respectively; d) and d') non-target objects.

3185 digital images were acquired, of which 1806 were YST images and 1380 were BST images. The images were 5184×3456 pixels (72 dpi) in the RGB color model.

2.2. Insect identification algorithm

The insect identification algorithm was applied in three stages. First, the algorithm preformed the detection of the objects by processing the region of interest of the trap image and returned a sample image for each object (Section 2.2.1). After this stage, the algorithm computed the subsequent processes, depending on the target insect. A segmentation algorithm processed each sample image (Section 2.2.2) to obtain an isolated object. Subsequently,

the morphological and color features of the isolated object were calculated. Finally, a feature classification was performed by a feed-forward artificial neural network (Section 2.2.3).

2.2.1. Algorithm to detect objects in trap images

Object detection in the digital images of the sticky trap was performed with a series of subroutines (Fig. 2). First, the region of interest (Fig. 1) was cropped from the sticky trap image. Next, the histogram for each channel of the RGB image within the region of interest was calculated. For each channel, intensity values of the pixels with a frequency greater than 10,000 were set as trap background (Fig. 3). As a result of the weekly sampling strategy, the frequency of the intensity values of pixels in the digital images for the target insects and other non-target objects never reached the predefined threshold of 10,000 in this experiment. Based on the frequency threshold value, intensity threshold values for each channel were determined to detect the background in the image.

Next, a binary image was created from each RGB channel based on the previously calculated intensity threshold values. Pixels on the channel outside the background intensity range were classified as objects. A logical disjunction was performed with the three binary channels to obtain a background mask image. Regions of pixels in the complementary image of the mask were filled up to obtain solid objects. Based on the distribution of the sampled areas for whiteflies and thrips (Fig. 4), only solid objects with an area from 50 to 2000 pixels were selected.

For each of the detected objects, a rectangular region of interest measuring 41×41 pixels was cropped by using the calculated centroid of the

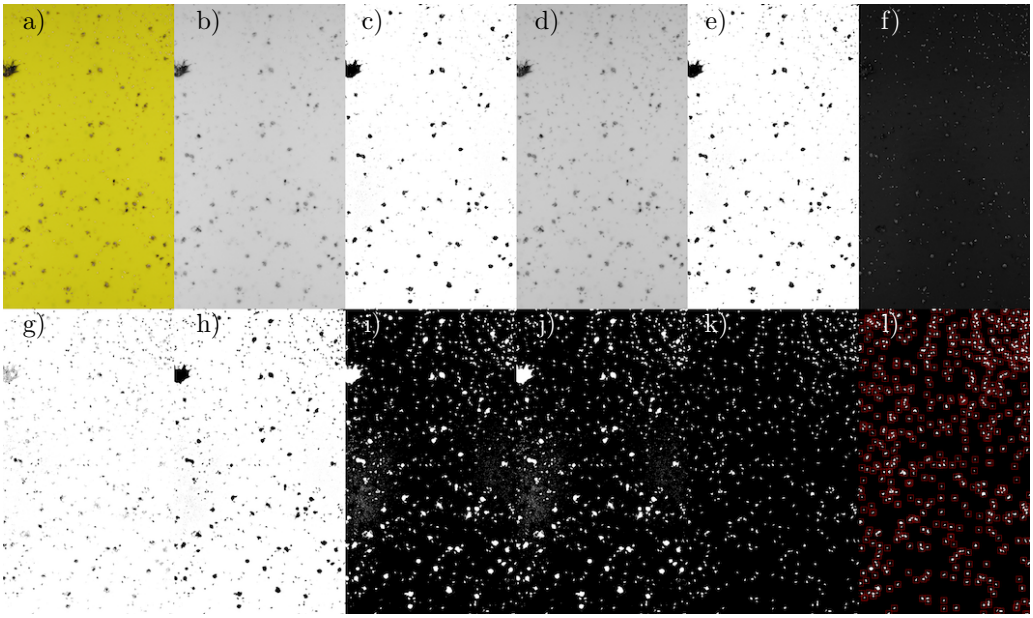

Figure 2: Object detection by image processing. a) RGB image of the region of interest; b), d) and f) R, G and B channels of the image, respectively; c), f) and g) segmentation of the R, G and B channels, respectively, based on pixel frequency; h) disjunction operation of c), e) and g); i) complementary image of h); j) image after filling-up object gaps for each region of pixels; k) selected objects by areas; l) calculated centroids for each object.

detected object as the center of the region of interest. This cropped image was then refferred to as sample image. After this process, two sets of randomly permuted sample images (32,844 and 32,700 from yellow and blue sticky trap, respectively) were divided in half to train the ANN and validate the insect identification algorithm.

2.2.2. Image segmentation and features extraction of the sample images

To identify whiteflies on the yellow sticky trap, an image segmentation algorithm (Fig. 5) was used to process each sample image. First, images were converted from RGB to *Lab* model (lightness (L) and the a and b color-

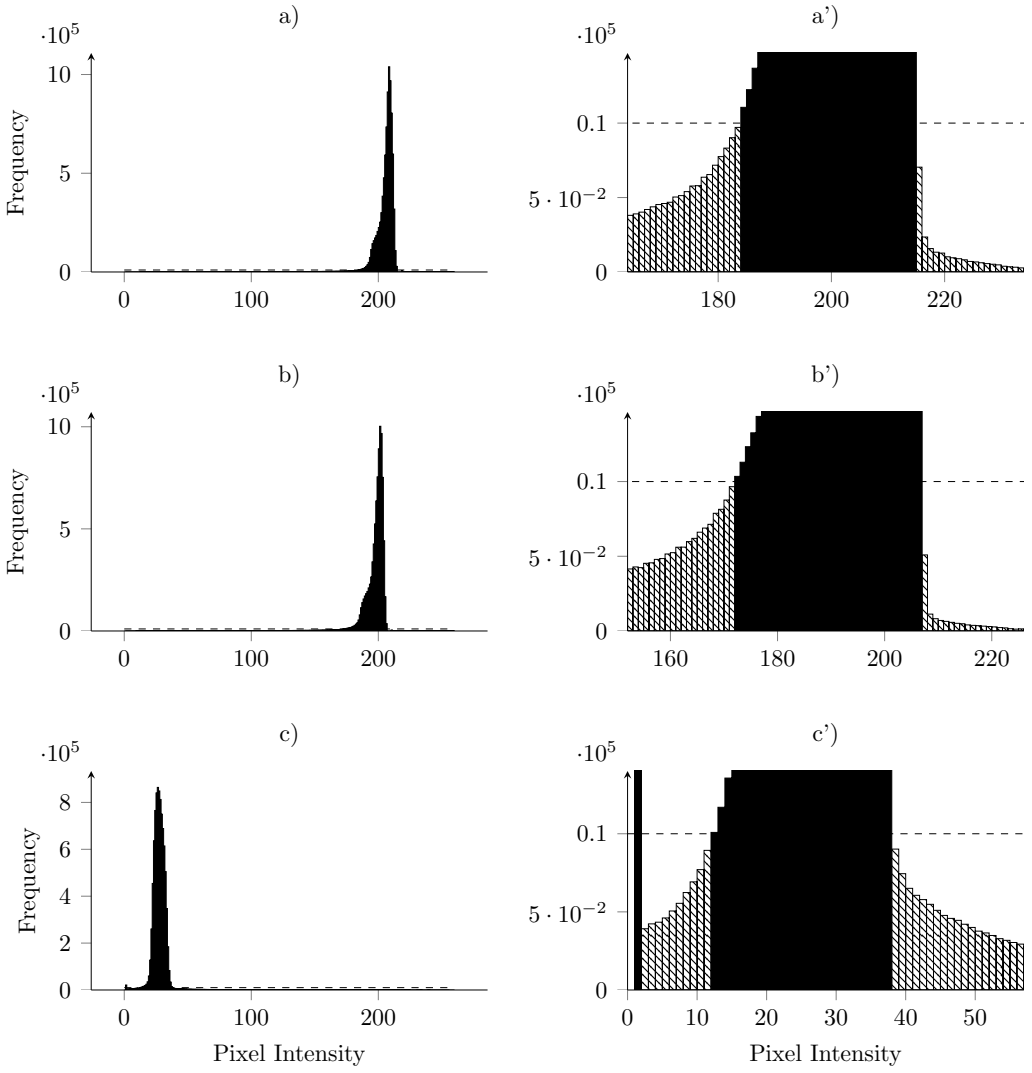

Figure 3: Histogram of the region of interest of a YST image. a), b) and c) Histograms of the R, G and B components, respectively. a'), b') and c') Details of the frequency threshold for each corresponding color component. (■) and (▧) frequencies values of the pixel intensities classified as background and objects, respectively; (- - -) frequency threshold value for the classification of background pixels and objects on the trap image.

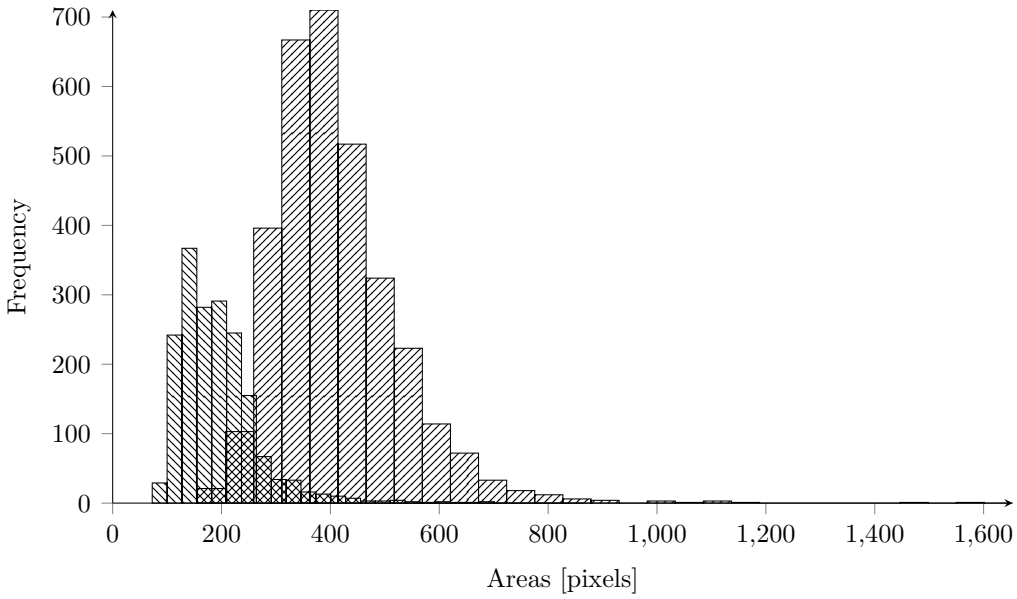

Figure 4: Histogram of target insect areas. ▨ Histogram of whitefly areas and ▧ histogram of thrip areas.

opponent dimensions). Then, for the a and b channels, a contrast stretch was performed by mapping the intensity values so that 1 % of the data at low and high intensities of the channels was saturated. Second, since the body and wings of the whitefly are mainly brown and white, respectively, separate segmentations were performed. The body was identified by using the a channel, while the wings were identified via the b channel. Automatic identification of the intensity threshold values was then implemented (Otsu, 1979) on each channel and a logical conjunction operation was performed. The connected components were then calculated with the previously computed binary image by using a 4-connected neighborhood pixel connection algorithm to obtain labeled regions of pixels. Subsequently, the morphological features (area, convex area, eccentricity, equivalent diameter, major axis

length, minor axis length, perimeter, centroid, solidity and extent) were calculated for each region of pixels. If more than one region was found in the sample image, only the region of pixels with the greatest area was considered as the object of interest. This last binary image of the resulting object was also used as a mask to determine the color features and the mean intensity value in each channel of the *Lab* color space.

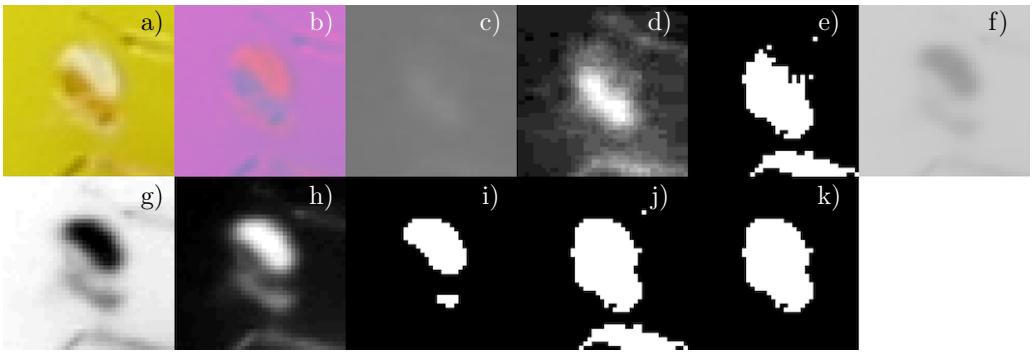

Figure 5: Image processing for whitefly identification. a) Original image in the RGB color model; b) *Lab* color model image; c) *a* component; d) contrast stretched image; e) binarization by using the Otsu Method; f) b component; g) contrast stretched image; h) complement of the image; i) binarization using the Otsu Method; j) logical conjunction operation of components *a* and *b*; k) selection of the objects with maximum area.

The image enhancement of the segmentation of the blue sticky trap image in Fig. 6 was performed by transforming the RGB image into an HSV color model. The same segmentation and morphological feature extraction was performed for the yellow sticky trap process, with the difference that only the saturation channel was segmented. In addition, the color features were extracted from the HSV image.

At the end of this process, the algorithm returned a vector containing 15 morphological and color features for each object. These were filtered based

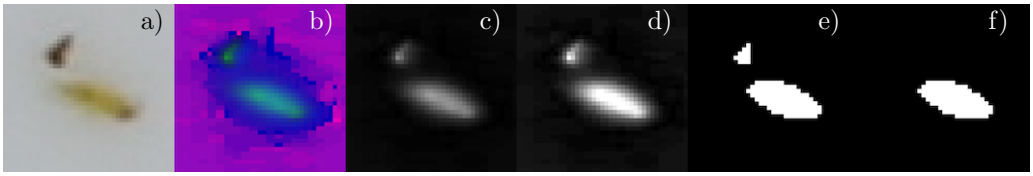

Figure 6: Image processing for thrip identification. a) Original sample image in the RGB color model; b) HSV image; c) saturation channel; d) contrast stretch image; e) binarization using the Otsu method; f) selection of the object with maximum area.

on the mutual information (Amjady et al., 2011) and only 14 were selected. Thus, the 14 elements in each vector, used as input of the neural network, were: area, convex area, eccentricity, equivalent diameter, major axis length, minor axis length, perimeter, solidity, extent, two components of the centroid and three mean color intensity values. On the one hand, each set of vectors (from yellow and blue sticky trap images, respectively) were manually and randomly permuted and divided in halves. The first half was used to design the neural network, while the validation of the automatic identification of the target insect from the sample images was performed based on the other half. For practical purposes, the two sets were referred to as Network Design Set (NDS) and Algorithm Validation Set (AVS). On the other hand, during the identifiaction of the target insect from the traps, the algorithm automatically used the resulting features of the segmentation process as input for the neural network.

2.2.3. Classification by a neural network

A multilayer feed-forward neural network (see Fig. 7) was used in this study to classify the detected objects using the extracted morphological and color features vector p_γ of length $R = 14$. The network consisted of a two-

layer perceptron (the input $\gamma = 1$ and the output $\gamma = 2$ layer) that processed the input signal with the log-sigmoid $f_{\gamma=1}(n) = \frac{1}{1+e^{-n}}$ and the line $f_{\gamma=2}(n) = n$ transfer functions, respectively. In order to find the optimum network configurations, 28 network configurations were trained. Thus, the number of nodes tested in these configurations was $S_{\gamma=1}/S_{\gamma=2} = [1 \text{ to } 28]/2$. In the network training, the output signal for a target insect vector and a non-target object were $a_{\gamma=2} = [1, 0]$ and $a_{\gamma=2} = [0, 1]$, respectively.

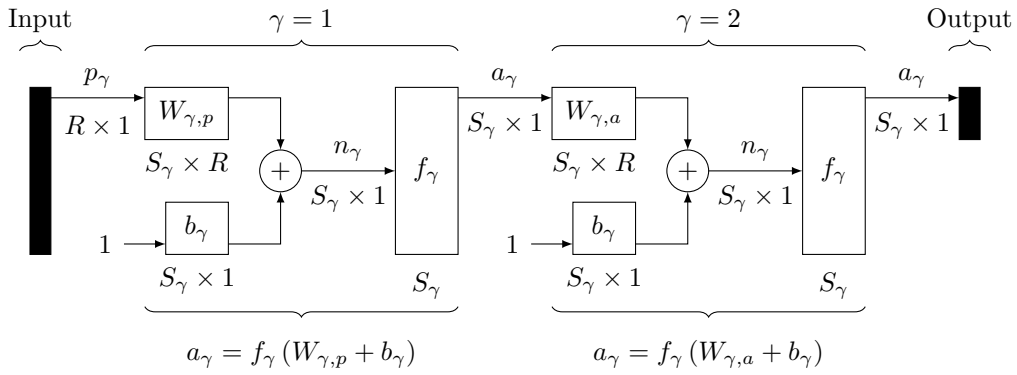

Figure 7: Multilayer artificial neural network architecture for whitefly and thrip features classification.

The NDS was randomly set aside in 70 % for training, 15 % for testing and 15 % for validation of the neural network. The Levenberg-Marquardt optimization method (Marquardt, 1963) was used to update weight W and bias b values in the training process. A bias enhanced the net input of the transfer function, depending on whether it is positive or negative, respectively (Haykin, 1998). The process was stopped if the validation error increased after 10 iterations, or if the mean square error of the validation reached a minimum of 0.01. Then, the weights W and biases b calculated at the minimum error of the validation were used as values for the network validation

with a new set of input vectors.

The balance of the elements in the output signal $a_{\gamma=2}$ was measured by using the expression $a_b = a_{\gamma=2}(1) - a_{\gamma=2}(2)$, resulting in a new a_b output signal. In this signal, the positive values are considered the target insects and the negative values are the non-target objects. In this paper, this qualitative classification output is refferred to as a_c for practical purposes.

The networks were first validated with the qualitative output signal a_c using AVS to find the optimum neural network. After the analysis of all the samples S_a in AVS, a_c contained the identified target insects I_{ti} and non-target objects I_{nt} of length S_{ti} and S_{nt}, respectively. With these parameters, the mean absolute error (MAE) was estimated and the precision P_{nn} of the neural network was calculated as:

$$P_{nn} = \frac{S_a - MAE}{S_a} \times 100 \tag{1}$$

The identification error, false negative rate (FNR) and false positive rate (FPR) were:

$$FNR = \frac{\sum I_{ti-nn}}{S_{ti}} \times 100 \tag{2}$$

$$FPR = \frac{\sum I_{nt-nn}}{S_{nt}} \times 100 \tag{3}$$

After finding the best network with the previous analysis, a quantitative analysis with the a_b output signal was performed. Subsequently, the root mean square error (RMSE), the RMSE-observations standard deviation ratio (RSR), the percentage of the error bias (PBIAS), the absolute error (MAPE) and the linear correlation (Kobayashi and Salam, 2000; Moriasi et al., 2007)

were calculated to compare both networks designed to identify whiteflies and thrip.

2.3. Validation of the algorithm

Two types of evaluations of the identification system were performed to measure the performance of the algorithm: identification of the target insect from the trap images and from the sample images.

The identification of the target insects from trap images was performed using traps with low insect density per trap. It is important to analyze the performance of the automatic identification system in this domain because maintaining low infestation is a crucial objective in an IPM system. Park et al. (2007) suggested an economic threshold of 5.7 thrip per four-day sticky trap count, whereas Ellsworth and Martínez-Carrillo (2001) reported a maximum threshold of 10 whiteflies per leaf to perform corrective actions and prevent crop infestation. As a result of the implementation of pest management in the experimental greenhouses, mean target insects captured per trap were 3.7 for YST and 2.7 for BST. Thus, we processed 1731 YST images and 1348 BST images that provided a density below 30 insects per trap. The procedure proposed by Altman and Bland (1983) was used to assess the magnitude of disagreement (both error and bias) between the identification system and the measured values.

The performance of the algorithm to identify the target insect in the sample images was measured calculating the precision, the recall and the F-measure for both target insects, whitefly and thrip. To determine these parameters, the number of observed target insects was used as our reference (N) and the number of automatic identified target insects as our hypothesis

(M). These values were determined as follows (Makhoul et al., 1999):

$$N = C + B + D \tag{4}$$

$$M = C + B + I \tag{5}$$

where C is the number of correctly identified target insects, B the number of substitutions, I the number of deletions and D the number of insertions.

Precision P and recall R are commonly used to measure the performance of information retrieval and information extraction systems (Makhoul et al., 1999) as well as in those algorithms developed for pest identification (Kumar et al., 2010; Zhao et al., 2011b; Xia et al., 2014; Yan et al., 2015). Precision is related to substitution and insertion errors and can be considered a measure of exactness or fidelity, while recall is a measure of completeness that is related to substitution and deletion errors. These parameters were calculated as (Makhoul et al., 1999):

$$P = \frac{C}{M} \tag{6}$$

$$R = \frac{C}{N} \tag{7}$$

Subsequently, the weighted harmonic mean of the precision and recall (F-measure) was determined (Makhoul et al., 1999) to determine the overall performance of the insect identification algorithm, including miss detection and false alarms:

$$F = \frac{2 \times P \times R}{P + R} \tag{8}$$

3. Results and discussion

The experimental results are based on two main analyses. First, the results of the three image processing stages (object detection, segmentation and features extraction) will be reviewed, followed by an analysis of the feature classifications using a neural network. Both processes are important because they contribute to the final efficiency of the insect identification.

Although the purpose of this paper is not to evaluate the effect of abiotic factors and agrosystem management in the performance of the insect identification algorithm, the sampling methodology or to analyze insect population dynamics, it is important to note that the insect sampling methodology and the image acquisition system provided a large quantity of representative experimental data.

3.1. Object detection subroutine

As an alternative to the methods used to optimize the information to be processed discussed in Section 1, we found that by using the object detection subroutine proposed in this study, most information in the trap images refered to the background (95.13 %), which is not relevant in the insect identification process and can be neglected. An average of 268.78 ± 195.76 objects per trap represented 4.87 ± 3.55 % of the trap image that contained information about the objects stuck to the trap and this fraction of data was used to identify the target insects. In the most infested trap (1414 detected objects) the extracted information was 25.60 %, while the percentage for the minimum infestation (10 objects) was 0.18 %. Considering that in an agrosystem managed with an early pest detection strategy, high infestation is prevented by

increasing pest population monitoring frequency (Pinto-Zevallos and Vänninen, 2013), the density of the captured objects in the sticky trap will also be lowered. Thus, the fewer objects captured in the trap, the more background information that can be neglected. The object detection subroutine used in this study was effective in detecting the target classes, i.e. whiteflies, thrips and other objects, but it can also be applied to the detection of other insect species. Nevertheless, improvements are still needed, since in some cases regions of pixels with areas greater than 800 pixels were detected, corresponding to insects that were degraded, overlapping, or located close to the frame shadow. Moreover, any object near a target insect appeared as a similar sample image because of the proximity of their centroids.

Since the object detection algorithm detected the background in accordance with a pixel frequency threshold, it was not sensitive to the color differences that it was evaluating (yellow and blue sticky traps). This also holds true for the variations in trap color intensity due to different conditions: light conditions in the acquisition system, trap degradation or trap manufacture. Using this subroutine, 662,011 and 194,060 objects were detected in the YST and BST images, respectively. From this amount, 6498 image samples of whiteflies and 26,346 image samples of non-whitefly objects, which included other insect species as well as other non-insect objects, were selected manually from the YST images. Likewise, 3589 image samples of thrips and 29,111 image samples of non-thrip objects were also selected manually from the BST images.

3.2. Image-processing subroutine

The sample image segmentation for whitefly identification was precise despite changes in color background, orientation or positioning of insect body parts (Fig. 8 a and b). Nevertheless, segmentation of detected objects located next to the boundary of the trap, near the steel frame (Fig. 1), generated erroneous results (Fig. 8 c'), due to the fact that the shadow produced by the frame changed the background color of the sample image (Fig. 8 c). In addition, if overlapping occurred (Fig. 8 d), both the whitefly and the other object were classified as a unique region of pixels (Fig. 8 d'). It is difficult to measure insect degradation, but also it affects insect identification performance.

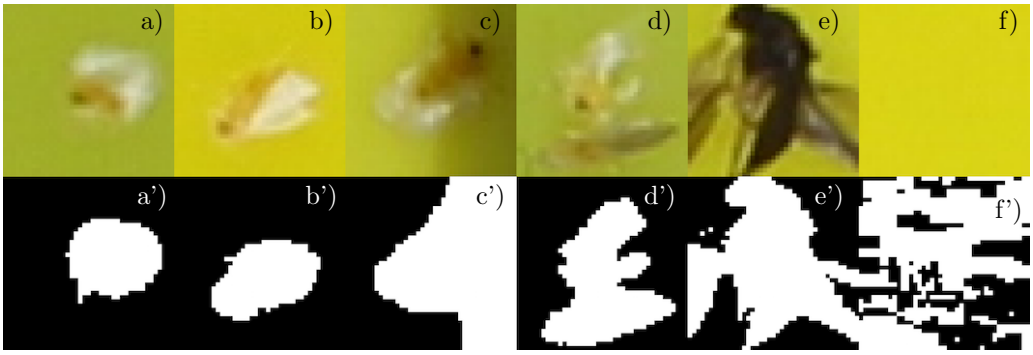

Figure 8: Main sample anomalies for whitefly identification. a) and b) background and body position and orientation differences; a') and b') image segmentation of images a) and b), respectively; c) and c') sample showing a frame shadow and the corresponding image segmentation, respectively; d) and d') sample showing a whitefly close to other non-target insect and its corresponding image segmentation; e) and e') non-target insect and its segmentation; f) and f') clean sample and its segmentation, respectively.

On the other hand, image segmentation for thrip identification was mostly a less challenging task. Background color differences, variation in orientation

and position of the insects, boundary shadows and overlapping were, in most cases, correctly segmented (see Fig. 9).

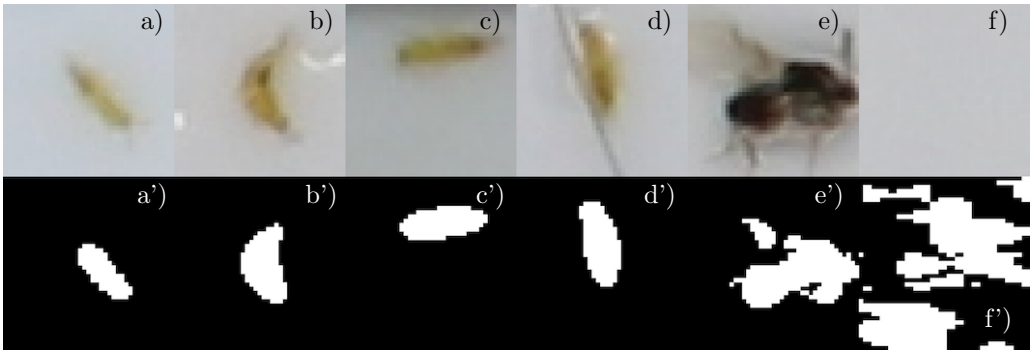

Figure 9: Main sample anomalies for thrip identification. a) and b) background and body position and orientation differences; a') and b') image segmentation of images a) and b), respectively; c) and c') sample showing a frame shadow and the corresponding image segmentation, respectively; d) and d') sample showing a thrip close to other non-target insect and its corresponding image segmentation; e) and e') non-target insect and its segmentation; f) and f') clean sample and its segmentation, respectively.

As in previous studies, the automatic identification of thrips was based on the use of blue sticky traps. We obtained satisfactory results by using the saturation channel of the HSV color model to identify thrip on the blue sticky trap. On the other hand, we proposed whitefly identification on the yellow sticky traps to be carried out in the a and b channels of the Lab color model. In other studies, whitefly identification on yellow sticky traps was performed on the C_b of the YC_bC_r color model (Xia et al., 2014) by using an *ad hoc* transformation from RGB to gray (Qiao et al., 2008; Solis-Sánchez et al., 2009; Bechar et al., 2010) or by processing the YUV color model (Cho et al., 2007).

By using the selected channels, the segmentation in both algorithms was

based on contrast adjustment and on the Otsu method (Otsu, 1979). This method was also used by Solis-Sánchez et al. (2009) to identify whitefly on yellow sticky traps. Both the whitefly and the thrip identification algorithms also segmented those pixel regions that were not objects of interest for the identification (i.e., sample images c and d in Fig. 8 and Fig. 9). Nevertheless, the overall performance of the algorithm depended not only on the morphological features used to classify the object, but also on color properties. As in recent studies (Barbedo, 2014; Xia et al., 2014), in this work, we demonstrate that morphological and color features are effective parameters to classify pest species captured in sticky traps. Main color component features calculated for whiteflies (Table 1) were similar to those reported by Cho et al. (2007), except in the green component, where these authors used 214 ± 13 as the domain to classify a whitefly, while this component was 117 ± 3 in our system. The eccentricity and solidity domains obtained with our system are similar to the values reported by Solis-Sánchez et al. (2009, 2011) to classify whitefly and thrip (0.85 ± 0.10 and 1, respectively). In our system, most of the calculated mean features (Table 1) were similar between target and non-target insects, and the dispersion of the values for each feature is high. A single feature could not be used in the classification process due to the fact that the separation between its values was not significant. This means that there was a high correlation between some classes. Under these conditions, artificial neural networks can be used to identify target insects.

3.3. Neural network for the classification of target insects

The results obtained for the 28 neural network procedures that were studied allowed the identification of the optimum neural network to identify each

Table 1: Mean observed features. TI and NTO are target insect and non-target object, respectively. Values are expressed as mean value ± standars deviation. * Mean component of the *Lab* color model calculated for whitefly or HSV color model calculated for thrip.

	Whitefly		Thrip	
Feature	TI	NTO	TI	NTO
Area	953 ± 512	868 ± 506	688 ± 442	698 ± 448
Centroid X	20.59 ± 4.67	20.40 ± 4.78	21.18 ± 5.93	21.21 ± 5.67
Centroid Y	19.75 ± 6.78	18.34 ± 7.35	23.62 ± 7.53	20.66 ± 8.03
Convex Area	1209 ± 559	1117 ± 567	933 ± 545	951 ± 558
Eccentricity	0.55 ± 0.27	0.60 ± 0.28	0.72 ± 0.19	0.70 ± 0.21
Equivalent diameter	33.10 ± 10.84	31.44 ± 10.82	27.65 ± 10.52	27.88 ± 10.53
Extent	0.70 ± 0.18	0.67 ± 0.18	0.62 ± 0.14	0.62 ± 0.15
Major axis length	44 ± 9	43 ± 9	41 ± 12	41 ± 11
Minor axis length	34 ± 14	32 ± 14	27 ± 13	27 ± 13
Perimeter	195 ± 77	186 ± 77	168 ± 78	173 ± 82
Solidity	0.77 ± 0.13	0.76 ± 0.13	0.74 ± 0.12	0.73 ± 0.12
Color component 1*	201 ± 14	183 ± 27	0.54 ± 0.15	0.52 ± 0.15
Color component 2*	117 ± 3	115 ± 4	0.08 ± 0.12	0.07 ± 0.09
Color component 3*	199 ± 7	193 ± 11	0.75 ± 0.07	0.73 ± 0.09

target insect. We found that the best network setup for the whitefly identification was 16/2 and 9/2 for the thrip identification. It was observed that for this particular application, neural network precision remained stable even if more neurons were added at this layer. Hence, more neurons in $\gamma = 1$ did not result in a considerable decrease in error but caused, however, an increase of computational costs. The 16/2 network for whitefly identification obtained a calculated precision $P_{nn} = 98.21\%$, $FNR = 5.02\%$, $FPR = 0.99\%$ and

$MAE = 1.790\%$. On the other hand, in the 9/2 network for thrip identification we obtained $P_{nn} = 98.65\%$, $FNR = 3.99\%$, $FPR = 1.03\%$ and $MAE = 1.352\%$. These detection rates are satisfactory compared with the $(97.0 \pm 0.4)\,\%$ obtained in the algorithm developed by Qiao et al. (2008) and the 97 % obtained by Solis-Sánchez et al. (2009). In these analyses we also considered the identification of non-target objects. The FPR in the identification of these objects was smaller than the FNR calculated for the identification of the target insect because during the training of the neural network the synapsis weights and bias were adjusted not only following the more homogeneous set, but also the greater set. As can been seen in Table 1, most of the features in both sets (TI and NTO) overlap. In order to avoid false fositive results, the AVS input set used to train the network contained more non-target objects than target insects. As regards whitefly identification, the set had 3266 target insects and 13,156 non-target objects, while the thrip identification set was 1778 and 14,572 target and non-target objects, respectively. Therefore, the network provided a better performance when avoiding false positive results.

With the proposed neural network architecture we found that the optimum number of neurons S in $\gamma = 1$ was 16 and 9 for the identification of whitefly and thrip, respectively. The RMSE accomplished by these networks were 0.253 and 0.221, respectively. These results are admissible because they are less than half the standard deviation of the measured data, 0.399 and 0.311 for whitefly and thrip, respectively. If we compare these parameters based on the measured standard deviations (Singh et al., 2005), the RSR for network for whitefly identification was lower (0.316) than the network used

for classification of thrips (0.355). Nevertheless, the output signal in the whitefly identification indicated overestimation bias (PBIAS of $-1.012\,\%$), while the network for thrip identification is more accurate and has a low underestimation bias (PBIAS of $0.309\,\%$). Moreover, this overestimation bias resulted in a MAPE of $11.366\,\%$. On the other hand, the thrip identification MAPE was $7.93\,\%$. Simulation of the network model showed that the linear correlation for whitefly identification is slightly greater ($R^2 = 0.900$) than for thrip identification ($R^2 = 0.874$).

The distribution of the a_b output for each neural network can be seen in Fig. 10. Output of the neural network for whitefly identification was 0.830 ± 0.378, while the output identified as non-target object was -0.965 ± 0.189. A similar distribution was found for the output of the neural network for thrip identification, 0.799 ± 0.337 and -0.973 ± 0.187 for target insect and non-target object, respectively. Since we declare positive values of a_b as the target insect, negative values in the histogram are FNR. In the negative output declared as non-target object, positive values are FPR.

3.4. Validation of the algorithm

Results of the target insect identification in the traps are shown in Fig. 11. The Bland-Altman analysis for the identification of whitefly showed a mean bias of -1.84 ± 11.60 between the estimated values using the automatic identification and the manually measured values. This meant that, on average, the proposed algorithm overestimated the score by -1.84 ± 11.60, as regards the number of insects per trap. The limits of agreement were also wide, from 7.92 to -11.60, which meant an increase in the potential of a wrong insect-per-trap count. However, the method used to identify thrip only increased

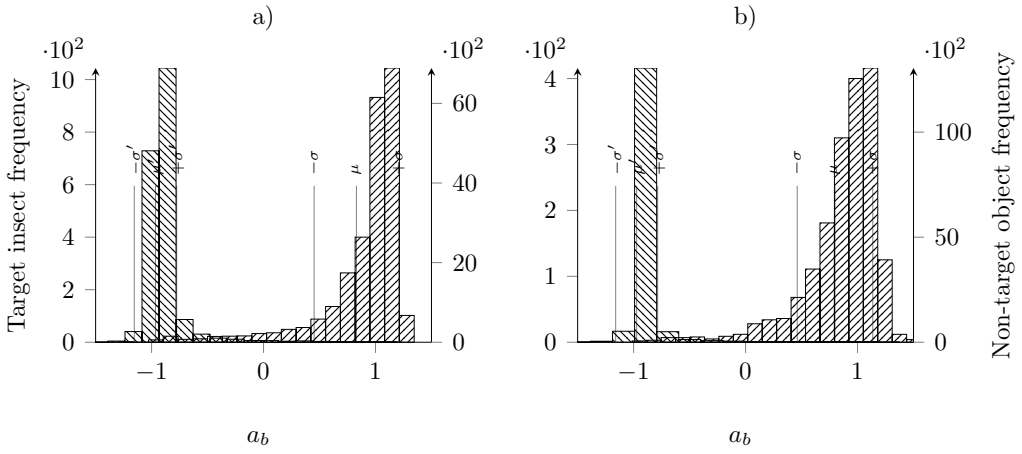

Figure 10: Neural networks validation results. a) and b) are the histograms of the whitefly and thrip identification, respectively; ▨ Target insects frequency; ▧ Non-target objects frequency; (μ, σ) and (μ', σ') are the mean and the a_b standard deviation output for target insect and non-target object, respectively.

the count on average by -0.59 ± 4.15, which indicates that this method is more trustworthy due to the narrow limits of agreement, from 3.56 to -4.74.

The performance parameters for target insect identification from the sample images are summarized in Table 2. The algorithm to identify whiteflies on the yellow-sticky traps provided higher precision (0.96) than the algorithm to identify thrips on the blue sticky traps (0.92). However, recall was marginally greater for identification of thrip (0.96) than for whitefly (0.95) as a consequence of a slightly greater tendency of the thrip identification algorithm to identify non-target objects as target insects. Both whitefly and thrip identification algorithms scored high F-measures, 0.96 and 0.94, respectively, indicating that correct identification instances exceeded incorrect

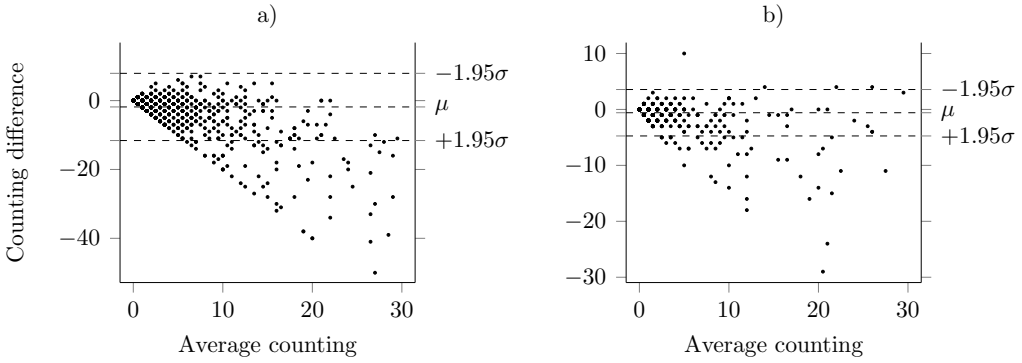

Figure 11: Mean-difference counting in traps with insect density < 30. a) and b) are the data ($\cdot$) of whitefly and thrip identification, respectively; μ is the mean difference and σ is standard deviation.

identifications.

Table 2: Performance parameters for the insect identification algorithm.

	Whitefly	Thrip
Observed value	3266	1778
Forecast	3232	1857
Correct forecast	3102	1707
Incorrect forecast	130	71
Insertions	34	0
Deletion	0	79
Precision	0.96	0.92
Recall	0.95	0.96
F-measure	0.95	0.94

Although the proposed identification system performs well when the identification of the target insect is performed from sample images, performance

quality drops in the object detection subroutine when it is used to identify the target insect from the traps. However, the insect identification system has a good correlation with the measured data when insect-per-trap density is low.

A comparison of these results with other published studies demonstrates that the combination of an image-processing algorithm with neural networks is a promising method for the future development of early pest detection systems using sticky traps. Barbedo (2014) reported for the identification of whitefly an F-measure value of 0.95 by using an image-processing algorithm. In another study, Yan et al. (2015) obtained an F-measure value of 0.89 for the *in situ* identification of whitefly by means of a multi-fractal minimal algorithm. Finally, Xia et al. (2014) reported a precision value of 0.96 in their image-processing algorithm for the identification of whitefly and thrip.

In this study, we have found that neural networks can be used to identify whitefly and thrip in sticky traps by using only 14 morphological and color features. Since the employed subroutine was designed to segment whitefly and thrip, the identification of further species requires a modification of the segmentation process. The improvement of the algorithm in terms of object detection and the segmentation process to identify a wider range of pest species will be the focus of a future work.

4. Conclusions

This study proposed a novel approach for the detection and quantification of adult-stage whitefly (*Bemisia tabaci*) and thrip (*Frankliniella occidentalis*) on sticky traps installed in greenhouses. The combination of the proposed

image-processing algorithm and the classification through artificial neural networks was explored as an algorithm model for the early detection and classification of the target insects. The identification system was based on the use of sticky traps, a commonly used physical method for capturing and monitoring pests in agriculture.

According to the experimental results, the developed algorithm model for adult whitefly identification from the sample images resulted in high precision (0.96), recall (0.95) and F-measure (0.95). Similar good performance was attained for the identification of adult thrip, with a value of 0.92 for precision, 0.96 for recall and 0.94 for F-measure.

Nevertheless, the proposed object detection subroutine caused a drop in the performance of the identification of the target insects from the trap. Future work will focus on the development of this subroutine, the detection of a wider range of insect species and the reduction of manual intervention.

Acknowledgements

This work has been funded by FEDER and the *Ministerio de Economía y Competitividad* (Government of Spain) by means of the research grant AGL2015-68050-R. The authors wish to express their gratitude to the Research Centre CIAIMBITAL of the University of Almería (Spain) and the National Council of Science and Technology (CONACYT) of Mexico, for their support through the development of this study. We would also like to thank Carlos Herrero for his thorough final revision of the manuscript.

5. Bibliography

Acebedo, M. M., May 2004. *Bemisisa tabaci*, una de las principales plagas en cultivos bajo abrigo. Vida Rural (189), 31–34, in Spanish

Altman, D. G., Bland, J. M. A., September 1983. Measurement in medicine: the analysis of method comparison studies. Journal of the Royal Statistical Society. Series D (The Statistician) 32 (3), 307–317

Amjady, N., Keynia, F., Zareipour, H., July 2011. Wind power prediction by a new forecast engine composed of modified hybrid neural network and enhanced particle swarm optimization. IEEE Transactions on Sustainable Energy 2 (3), 265–276

Anderson, M. D., Hollingsworth, C. S., Van Zee, V., Coli, W. M., Rhodes, M., December 1996. Consumer response to integrated pest management and certification. Agriculture, Ecosystems and Environment 60 (2-3), 97–106

Barbedo, J. G. A., December 2014. Using digital image processing for counting whiteflies on soybean leaves. J. Asia-Pac. Entomol. 17 (4), 685–694

Bauch, C., Rath, T., October 2005. Prototype of a vision based system for measurements of whitefly infestation. Acta Hortic. 691, 773–780

Bechar, I., Moisan, S., Thonnat, M., Bremond, F., August 2010. On-line video recognition and counting of harmful insects. In: 20th International Conference on Pattern Recognition (ICPR). IEEE, Istanbul, pp. 4068–4071

525 Biffi, A., September 2009. Development of an autonomous flying insect scout-
526 ing system for greenhouse environments. Master's thesis, Ohio State Uni-
527 versity

528 Boissard, P., Martín, V., Moisan, S., July 2008. A cognitive vision approach
529 to early pest detection in greenhouse crops. Comput. Electron. Agric.
530 62 (2), 81–93

531 CAPDR, 2014. Tomate - Delegación territorial de Almería. Tech. rep., Red
532 de alerta de información fitosanitaria, Consejería de Agricultura y Pesca,
533 Junta de Andalucía

534 Cho, J., Choi, J., Qiao, M., Ji, C.-w., Kim, H.-y., Uhm, K.-b., Chon, T.-s.,
535 2007. Automatic identification of whiteflies, aphids and thrips in green-
536 house based on image analysis. Int. J. Math. Comput. Simul. 1 (1), 46–53

537 Chung, B., Xia, C., Song, Y., Lee, J., Li, Y., Kim, H., Chon, T., Decem-
538 ber 2014. Sampling of *Bemisia tabaci* adults using a pre-programmed au-
539 tonomous pest control robot. J. Asia-Pac. Entomol. 17 (4), 737–743

540 Dhawan, A. K., Peshin, R., 2009. Integrated pest management: innovation-
541 development process. Vol. 1. Springer Netherlands, Dordrecht, Ch. Inte-
542 grated pest management: concept, opportunities and challenges, pp. 51–81

543 Ellsworth, P. C., Martínez-Carrillo, J. L., 2001. IPM for *Bemisia tabaci*: a
544 case study from North America. Crop Protection 20 (9), 853–869

545 Espinoza, K., Valera, D. L., Torres, J. A., López, A., Molina-Aiz, F. D.,
546 August 2015. An auto-tuning PI control system for an open-circuit low-

speed wind tunnel designed for greenhouse technology. Sens. 15 (8), 19723–19749

Gerling, D., Horowitz, A. R., July 1984. Yellow traps for evaluating the population levels and dispersal patterns of *Bemisia tabaci* (Gennadius) (Homoptera: Aleyrodidae). Ann. Entomol. Soc. of Am. 77 (6), 753–759

Ginoris, Y. P., Amaral, A. L., Nicolau, A., Coelho, M. A. Z., Ferreira, E. C., July 2007. Recognition of protozoa and metazoa using image analysis tools, discriminant analysis, neural networks and decision trees. Anal. Chim. Acta 595 (1-2 SPEC. ISS.), 160–169

Haykin, S., 1998. Neural networks: a comprehensive foundation, 2nd Edition. Prentice Hall PTR, Ontario canada

Heinz, K. M., Parrella, M. P., Newman, J. P., December 1992. Time-efficient use of yellow sticky traps in monitoring insect populations. J. Econ. Entomol. 85 (6), 2263–2269

Huddar, S. R., Gowri, S. S. S., Keerthana, K. H., Vasanthi, S., Rupanagudi, S. R., July 2012. Novel algorithm for segmentation and automatic identification of pests on plants using image processing. In: 2012 Third International Conference on Computing Communication & Networking Technologies (ICCCNT). Computing Communication & Networking Technologies, IEEE, Coimbatore, pp. 1–5

Isaacs, R., Byrne, D. N., December 1998. Aerial distribution, flight behaviour and eggload: their inter-relationship during dispersal by the sweetpotato whitefly. J. Anim. Ecol. 67 (5), 741–750

570 Kobayashi, K., Salam, M. U., March 2000. Comparing simulated and mea-
571 sured values using mean squared deviation and its components. Agronomy
572 Journal 92 (2), 345–352

573 Kumar, R., Martin, V., Moisan, S., 2010. Robust insect classification applied
574 to real time greenhouse infestation monitoring. In: Proceedings of the 20th
575 International Conference on Pattern Recognition on Visual Observation
576 and Analysis of Animal and Insect Behavior Workshop

577 Li, Y., Xia, C., Lee, J., July 2009. Vision-based pest detection and automatic
578 spray of greenhouse plant. In: ISIE 2009. IEEE International Symposium
579 on Industrial Electronics, 2009. IEEE, Seoul, pp. 920–925

580 López, A., Valera, D. L., Molina-Aiz, F. D., Peña, A., Marín, P., September
581 2013. Field analysis of the deterioration after some years of use of four
582 insect-proof screens utilized in Mediterranean greenhouses. Span. J. Agric.
583 Res. 11 (4), 958–967

584 López, A., Valera, D. L., Molina-Aiz, F. D., Peña, A. A., September 2012.
585 Sonic anemometry to evaluate airflow characteristics and temperature dis-
586 tribution in empty Mediterranean greenhouses equipped with pad fan and
587 fog systems. Biosyst. Eng. 113 (4), 334–350

588 Lowe, D. G., November 2004. Distinctive image features from scale-invariant
589 keypoints. Int J. Comput. Vis. 60 (2), 91–110

590 Makhoul, J., Kubala, F., Schwartz, R., Weischedel, R., 1999. Performance
591 measures for information extraction. In: In Proceedings of DARPA Broad-
592 cast News Workshop. pp. 249–252

Marquardt, D. W., June 1963. An algorithm for least-squares estimation of nonlinear parameters. J. Soc. Ind. Appl. Math. 11 (2), 431–441

Moriasi, D. N., Arnold, J. G., Van Liew, M. W., Bingner, R. L., Harmel, R. D., Veith, T. L., May 2007. Model evaluation guidelines for systematic quantification of accuracy in watershed simulations. Transactions of the ASABE 50 (3), 885–900

Otsu, N., January 1979. A threshold selection method from gray-level histograms. IEEE Trans. Syst. Man Cybern. 9 (1), 62–66

Park, H., Lee, J., Uhm, K., March 2007. Economic thresholds of western flower thrips (*Thysanoptera: Thripidae*) for unripe red pepper in greenhouse. Journal of Asia-Pacific Entomology 10 (1), 45–53

Pérez, P., Gázquez, J. C., López, J. C., Baeza, E., Meca, D., Pérez, C., November 2010. Tecnología de invernaderos y control biológico - Técnicas de cultivo que afectan a la viabilidad del control biológico en los invernderos de Almería. Tech. Rep. CEA01, Fundación Cajamar, in spanish

Pinto-Zevallos, D. M., Vänninen, I., May 2013. Yellow sticky traps for decision-making in whitefly management: What has been achieved? Crop Prot. 47 (0), 74–84

Qiao, M., Lim, J., Ji, C. W., Chung, B.-K., Kim, H.-Y., Uhm, K.-B., Myung, C. S., Cho, J., Chon, T.-S., March 2008. Density estimation of *Bemisia tabaci* (Hemiptera: Aleyrodidae) in a greenhouse using sticky traps in conjunction with an image processing system. J. Asia-Pac. Entomol. 11 (1), 25–29

Singh, J. P. A., Knapp, V. V., Arnold, J. G., Demissie, M., April 2005. Hydrological modeling of the iroquois river watershed using hspf and swat. Journal of the American Water Resources Association 41 (2), 343–360

Solis-Sánchez, L. O., Castañeda Miranda, R. C. n., García-Escalante, J. J., Torres-Pacheco, I., Guevara-González, R. G., Castañeda Miranda, C. L., Alaniz-Lumbreras, P. D., January 2011. Scale invariant feature approach for insect monitoring. Comput. Electron. Agric. 75 (1), 92–99

Solis-Sánchez, L. O., García-Escalante, J. J., Castañeda Miranda, R. C. n., Torres-Pacheco, I., Guevara-González, R. G., February 2009. Machine vision algorithm for whiteflies (*Bemisia tabaci* Genn.) scouting under greenhouse environment. J. Appl. Entomol. 133 (7), 546–552

Steiner, M. Y., Spohr, L. J., Barchia, I., Goodwin, S., November 1999. Rapid estimation of numbers of whiteflies (Hemiptera: Aleurodidae) and thrips (Thysanoptera: Thripidae) on sticky traps. Aust. J. of Entomol. 38 (4), 367–372

Tang, S., Xiao, Y., Chen, L., Cheke, R. A., June 2005. Integrated pest management models and their dynamical behaviour. Bull. Math. Biol. 67 (1), 115–135

Teitel, M., Tanny, J., Ben-Yakir, D., Barak, M., November 2005. Airflow patterns through roof openings of a naturally ventilated greenhouse and their effect on insect penetration. Biosyst. Eng. 92 (3), 341–353

637 Valera, D. L., Álvarez, A. J., Molina-Aiz, F. D., October 2006. Aerodynamic
638 analysis of several insect-proof screens used in greenhouses. Span. J. Agric.
639 Res. 4 (4), 273–279

640 Valera, D. L., Belmonte, L. J., Molina-Aiz, F. D., López, A., June 2016.
641 Greenhouse agriculture in Almería. A comprehensive techno-economic
642 analysis. No. 21 in Economía. Cajamar Caja Rural

643 Wise, J. C., Gut, L. J., Isaacs, R., 2015. Michigan fruit management guide.
644 Tech. rep., Department of Plant Pathology and Department of Horticul-
645 ture, Michigan State University

646 Xia, C., Chon, T., Ren, Z., Lee, J., September 2014. Automatic identifica-
647 tion and counting of small size pests in greenhouse conditions with low
648 computational cost. Ecol. Inform. 29 (2), 139–146

649 Yaakob, S. N., Jain, L., July 2012. An insect classification analysis based on
650 shape features using quality threshold ARTMAP and moment invariant.
651 Appl. Intell. 37 (1), 12–30

652 Yan, L., Chunlei, X., Jangmyung, L., October 2015. Detection of small-sized
653 insect pest in greenhouses based on multifractal analysis. Int. J. Light and
654 Electron Opt. 126 (19), 2138–2143

655 Zhao, J., Zheng, F., Wang, Y., Ye, B., Zhao, X., Mu, H. Y., Hao, L. W.,
656 2011a. Geostatistical analysis of spatial patterns of *Bemisia tabaci* (Ho-
657 moptera: Aleyrodidae) adults in tobacco field. In: 6th IEEE Conference
658 on Industrial Electronics and Applications (ICIEA). pp. 2394–2398

659 Zhao, X., Satoh, Y., Takauji, H., Kaneko, S., Iwata, K., Ozaki, R., June
660 2011b. Object detection based on a robust and accurate statistical multi-
661 point-pair model. Pattern Recognit. 44 (6), 1296–1311